NONLINEAR PROCESSES

M.V. TKACH, JU.O. SETI, JU.B. GRYNYSHYN

Yu. Fed'kovich National University of Chernivtsi
(2, Kotsyubyns'kyi Str., Chernivtsi 58012, Ukraine; e-mail: ktf@chnu.edu.ua)

INFLUENCE OF CONFINED POLARIZATION PHONONS ON THE ELECTRON SPECTRUM IN THE THREE-BARRIER ACTIVE ZONE OF A QUANTUM CASCADE DETECTOR

The Hamiltonian of an electron-phonon system in the second-quantization representation for all variables has been obtained. The models of effective mass and rectangular potentials for electrons and the polarization continuum model for confined phonons in a three-barrier resonant tunneling nanostructure are used. In the framework of the Green's function method, the phonon-renormalized electron spectra are calculated for a three-barrier resonant tunneling nanostructure composed of GaAs wells and $Al_x Ga_{1-x} As$ barriers with various Al contents x's. Irrespective of the Al content, the temperature-induced variations in the geometrical configuration of the three-barrier resonant tunneling nanostructure within the temperature interval from 0 to 300 K are found to increase the widths of both lower (working) quasi-stationary states and decrease their energies. The widths and the shifts of the states turned out to be strongly nonlinear functions depending on the position of the internal barrier in the three-barrier resonant tunneling nanostructure.

K e y w o r d s: resonant tunneling nanostructure, quantum cascade detector, electron-phonon interaction.
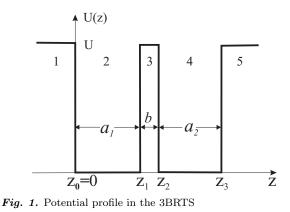
1. Introduction

Nano-dimensional heterostructures have been intensively studied recently, since they are basic elements for unique nanodevices, such as quantum cascade lasers (QCLs), quantum cascade detectors (QCDs), and so forth, which operate on the basis of novel physical effects that arise in multilayered nanostructures of the general type and, in particular, in resonant tunneling ones. It is the electron transport through open multilayered resonant tunneling structures (RTSs) that provides the functioning of QCLs and QCDs, which are studied in detail both experimentally [1–7] and theoretically [8–12]. Concerning QCDs, they were created to operate and mainly operated at cryogenic temperatures. However, a considerable progress has been achieved since then in understanding the physical processes occurring in nano-RTSs, which made it possible to substantially expand the temperature interval where those nanodevices can successfully function [13].

The temperature dependences of physical parameters for any system are basically governed by the interaction of major quasiparticles – in particular, electrons – with phonons. Therefore, theoretical researches of the electron-phonon interaction in nanoheterosystems with various dimensionalities and geometrical shapes attracted considerable attention [14–16].

Concerning planar nanostructures, the overwhelming majority of theoretical works dealing with them were devoted to the analysis of the electron-phonon interaction in closed two- and three-barrier RTSs (3BRTSs) with fixed geometrical parameters. Various

Fig. 1. Potential profile in the 3BRTS

methods were used to study their current-voltage characteristics and the probabilities of quantum transitions stimulated by an electromagnetic field making allowance for the electron-phonon interaction [17, 18]. As the main model of electron-phonon interaction in those works, the model of dielectric continuum was selected, which was developed in detail for the first time by Mori and Ando [19]. In work [19], the interaction Hamiltonian for the so-called binary heterosystems was presented in the coordinate representation for electron variables and the second-quantization representation for phonons. Later, this approach was extended onto three-component systems [20, 21]. The basic theoretical researches were carried out using the Fermi golden rule. The latter made it possible to calculate and analyze the temperature evolution of parameters that characterize interband quantum transitions [17, 18, 21]. However, it did not allow one to find how the electron-phonon interaction modifies the energies and the damping of quasi-stationary electron states in quantum-well RTSs.

This work aimed at obtaining an explicit expression for the Hamiltonian of a system of electrons that interact with confined polarization phonons in the second-quantization representation for all system variables. This expression allows the method of temperature electron Green's functions to be used in order to calculate the renormalization of the spectral parameters (shifts and damping) of quasi-stationary states in opened 3BRTSs with sufficiently high external barriers, which serve as the active zones of experimental QCDs [22, 23], and analyze the evolution of those parameters depending on the geometrical design, the Al content x, and the temperature of the

system T. As an example, we took a typical RTS on the basis of GaAs wells and $Al_xGa_{1-x}As$ barriers.

2. Theory of Interaction Between Electrons and Confined Polarization Phonons in 3BRTSs

2.1. Energy spectrum, wave functions, and Hamiltonian of electrons in the second-quantization representation

The thickness of external layers in a three-barrier RTS used as active zones in experimental QCDs is rather large (3–6 nm) [13]. Therefore, while developing the theory of electron-phonon interaction, we use the model of closed 3BRTS (Fig. 1) with the known effective masses and the potential relief

$$m(z) = \begin{cases} m_w, \\ m_b, \end{cases} \quad U(z) = \begin{cases} 0, & \text{reg. 2, 4,} \\ U, & \text{reg. 1, 3, 5.} \end{cases} \quad (1)$$

Assuming the electron wave function to have the form

$$\Psi_{n\mathbf{k}}(\mathbf{r}) = \frac{1}{\sqrt{S}} e^{i\mathbf{k}\boldsymbol{\rho}} \Psi_n(z), \quad (2)$$

where $\mathbf{k}$ and $\boldsymbol{\rho}$ are the quasi-momentum and the radius vector, respectively, of an electron in the plane xOy, and S is the area of the main region in this plane, we obtain the following Schrödinger equation for the z-dependent factor $\Psi_n(z)$ of this function:

$$\left[-\frac{\hbar^2}{2} \frac{d}{dz} \frac{1}{m(z)} \frac{d}{dz} + U(z) \right] \Psi_n(z) = E_n \Psi_n(z). \quad (3)$$

The total energy of the electron, E, is determined by the sum

$$E_{n\mathbf{k}} = E_n + \frac{\hbar^2 \mathbf{k}^2}{2m_n^*}. \quad (4)$$

Here, the energy component in the plane perpendicular to the axis Oz is determined, as was done in work [17], by the effective electron mass in the n-th subband correlated over the RTS,

$$\frac{1}{m_n^*} = \int_{-\infty}^{\infty} \frac{|\Psi_n(z)|^2}{m(z)} dz, \quad (5)$$

where $\Psi_n(z)$ and E_n are determined by the solutions of Eq. (3);

$$\Psi_n(z) = \sum_{j=1}^{5} \Psi_{jn}(z) =$$

$$= \begin{cases} \sum\limits_{j=2,4} (A_{jn}\cos k_n z + B_{jn}\sin k_n z); \\ \sum\limits_{j=1,3,5} (A_{jn}\mathrm{e}^{\chi_n z} + B_{jn}\mathrm{e}^{-\chi_n z}); \end{cases} \qquad (6)$$

$$k_n = \hbar^{-1}\sqrt{2m_w E_n}; \chi_n = \hbar^{-1}\sqrt{2m_b(U - E_n)} =$$

$$= \sqrt{2m_b U\hbar^{-2} - k_n^2 m_b/m_w}. \qquad (7)$$

Under the condition that the wave function vanishes as $z \to \pm\infty$, we obtain $B_{1n} = A_{5n} = 0$, whereas the other A_{jn} and B_{jn} coefficients and the energy spectrum E_n are unequivocally determined by the boundary conditions

$$\Psi_{jn}(z)|_{z=z_j} = \Psi_{j+1n}(z)|_{z=z_j}; \quad j = 1\text{–}4;$$

$$\frac{1}{m_j}\frac{d\Psi_{jn}(z)}{dz}\Big|_{z=z_j} = \frac{1}{m_{j+1}}\frac{d\Psi_{j+1n}(z)}{dz}\Big|_{z=z_j}, \qquad (8)$$

and the normalization condition

$$\int\limits_{-\infty}^{\infty} \Psi_n^*(z)\Psi_{n'}(z)dz = \delta_{nn'}. \qquad (9)$$

Changing to the second-quantization representation for the quantized wave function in the electron Hamiltonian,

$$\hat{\Psi}(\mathbf{r}) = \sum_{n,\mathbf{k}} \Psi_{n\mathbf{k}}(\boldsymbol{\rho}, z)a_{n\mathbf{k}}, \qquad (10)$$

we obtain the Hamiltonian of noninteracting electrons in the occupation-number representation:

$$\hat{H}_e = \sum_{n,\mathbf{k}} E_{n\mathbf{k}}a_{n\mathbf{k}}^+ a_{n\mathbf{k}}, \qquad (11)$$

where the electron spectrum $E_{n\mathbf{k}}$ is defined by formula (4), and the fermionic operators of creation $(a_{n\mathbf{k}}^+)$ and annihilation $(a_{n\mathbf{k}})$ of the electron state satisfy the anticommutation relations.

2.2. Hamiltonians of confined phonons and electron-phonon interaction

It is well known [17, 24] that, in the framework of the dielectric continuum model, the spectra of interface and confined phonons and the potentials of their polarization fields are determined by the equation

$$\varepsilon_j(\omega)\nabla^2\Phi(\mathbf{r}) = 0, \qquad (12)$$

where $\varepsilon_j(\omega)$ is the dielectric permittivity of the j-th layer in a system of two or three different layers; respectively,

$$\varepsilon_j(\omega) = \varepsilon_{j\infty}\frac{\omega^2 - \omega_{Lj}^2}{\omega^2 - \omega_{Tj}^2};$$

$$\varepsilon_j(\omega) = \varepsilon_{j\infty}\frac{(\omega^2 - \omega_{Lj1}^2)(\omega^2 - \omega_{Lj2}^2)}{(\omega^2 - \omega_{Tj1}^2)(\omega^2 - \omega_{Tj2}^2)}. \qquad (13)$$

Here, $\varepsilon_{j\infty}$ is the high-frequency dielectric permittivity and ω_{Lj}, ω_{Lj1}, ω_{Lj2}, ω_{Tj}, ω_{Tj1}, and ω_{Tj2} are the frequencies of longitudinal (L) and transverse (T) vibrations in the j-th medium.

Equation (12) has solutions of two types, which, in the case of non-uniform nanoheterosystems are supplemented with boundary conditions determined at its every interface. If $\varepsilon_j(\omega) \neq 0$, we obtain $\nabla^2\Phi_I(\mathbf{r}) = 0$. Then, with regard for the conditions describing the continuity of the potential Φ_I and the induction of this field across every interface of the heterosystem, we find the polarization field of interface phonons (I-phonons). The quantization of this field determines the energy spectrum of I-phonons [21]. On the other hand, if $\nabla^2\Phi_L(\mathbf{r}) \neq 0$, we have $\varepsilon_j(\omega) = 0$. In this case, in view of the boundary conditions known from work [19], which are needed for the potential of the polarization field of confined phonons to disappear $(\Phi_{jL}(\boldsymbol{\rho}, z_j) = 0)$ at every nanoheterosystem interface–irrespective of whether the media are confined or semi-infinite, or whether they are two- or three-component materials–the energies of confined phonons in them are determined by the same frequencies as in massive materials, namely,

$$\Omega_j = \hbar\omega_{Lj}, \quad \Omega_{j\ell} = \hbar\omega_{Lj\ell}, \quad (\ell = 1, 2). \qquad (14)$$

The series expansion of the polarization field potential in the j-th medium in a two-dimensional Fourier series

$$\Phi_j(\boldsymbol{\rho}, z) = \sum_{\lambda,\ell,\mathbf{q}} \Phi_{j\ell\lambda}(\mathbf{q}, z)\mathrm{e}^{\mathrm{i}\mathbf{q}\boldsymbol{\rho}} \qquad (15)$$

followed by the change from the Fourier components, first, to the normal generalized coordinates and momenta and, then, to the occupation number operators according to the well-known quantum-mechanical procedure [16] brings us to the Hamiltonian of confined phonons in the model of three-

component material,

$$\hat{H}_L = \sum_{j,\ell,\lambda,\mathbf{q}} \Omega_{j\ell}(b_{j\ell\lambda\mathbf{q}}^+ b_{j\ell\lambda\mathbf{q}} + 1/2). \tag{16}$$

Note that hereafter the formulas are presented for a more general three-component model, in which the subscript ℓ accepts the values of 1 and 2. However, all formulas remain also valid for the two-component model (by putting $\ell = 1$). The operators $b_{j\ell\lambda\mathbf{q}}^+$ and $b_{j\ell\lambda\mathbf{q}}$ satisfy the bosonic commutation relations.

The mode normalization and the L-phonon field quantization in the framework of the dielectric continuum model were carried out for binary heterosystems in work [19] by Mori and Ando and for ternary ones in works [17, 20]. Hence, with regard for the potentials of polarization fields for the separate j-th medium known from works [17, 20], the Hamiltonian of electron interaction with all branches (λ) of confined and semi-confined phonons in the whole heterosystem in the second-quantization representation for the phonon variables can be written in the form

$$\hat{H}_{e-L} = - \sum_{j,\ell,\lambda,\mathbf{q}} \sqrt{\frac{8\pi\hbar e^2 d_j \left(\frac{\partial\varepsilon_j(\omega)}{\partial\omega}\big|_{\omega=\omega_{Lj\ell}}\right)^{-1}}{S(\pi^2\lambda^2 + q^2 d_j^2)}} \times$$
$$\times \left\{ \begin{array}{l} \cos\left[\pi\lambda\left(\frac{z-z_{j-1}}{d_j} - \frac{1}{2}\right)\right], \lambda = 1, 3, 5, ... \\ \sin\left[\pi\lambda\left(\frac{z-z_{j-1}}{d_j} - \frac{1}{2}\right)\right], \lambda = 2, 4, 6, ... \end{array} \right\} \times$$
$$\times H_j(z)e^{i\mathbf{q}\boldsymbol{\rho}}(b_{j\ell\lambda\mathbf{q}} + b_{j\ell\lambda\mathbf{q}}^+). \tag{17}$$

Here, $H_j(z)$ is the function

$$H_j(z) = \begin{cases} 1, & \text{if } z \text{ is in the } j\text{-th layer,} \\ 0, & \text{otherwise,} \end{cases} \tag{18}$$

introduced in work [19], $\mathbf{q}$ is the two-dimensional quasi-momentum of phonons, and d_j is the thickness of the j-th region.

Changing to the second-quantization representation in Hamiltonian (17) and using the quantized wave function of electrons (10), the Hamiltonian of e-L interaction in the occupation-number representation for the electron and phonon variables takes the form

$$\hat{H}_{e-L} = \sum_{n,n'} \sum_{j,\ell} \sum_{\lambda,\mathbf{q}} F_{n'n}^{j\lambda}(\ell, q) \times$$
$$\times a_{n'\mathbf{k}+\mathbf{q}}^+ a_{n\mathbf{k}}(b_{j\ell\lambda\mathbf{q}} + b_{j\ell\lambda\mathbf{q}}^+). \tag{19}$$

Here, the coupling functions look like

$$F_{n'n}^{j\lambda}(\ell, q) = f_{n'n}^{j\lambda}(\ell)\frac{d_j}{\sqrt{S}}(\pi^2\lambda^2 + q^2 d_j^2)^{-1/2}, \tag{20}$$

where the quantities

$$f_{n'n}^{j\lambda}(\ell) = -\sqrt{\frac{8\pi\hbar e^2}{d_j} \left(\frac{\partial\varepsilon_j(\omega)}{\partial\omega}\big|_{\omega=\omega_{Lj\ell}}\right)^{-1}} \times$$
$$\times \int_{z_{j-1}}^{z_j} dz\,\Psi_{jn'}^*(z)\Psi_{jn}(z) \times$$
$$\times \left\{ \begin{array}{l} \cos\left[\pi\lambda\left(\frac{z-z_{j-1}}{d_j} - \frac{1}{2}\right)\right], \lambda = 1, 3, 5, ... \\ \sin\left[\pi\lambda\left(\frac{z-z_{j-1}}{d_j} - \frac{1}{2}\right)\right], \lambda = 2, 4, 6, ... \end{array} \right\} \tag{21}$$

characterize the strength of the electron-phonon interaction.

The integral in Eq. (21), as is seen from formula (6), contains simple trigonometric and exponential functions. Therefore, although it can be written precisely in the analytical form, the latter is cumbersome and is not presented here. Note that the electron-I-phonon interaction is not considered here, because, first of all, this important theoretical problem demands a substantial growth of the work volume, which would exceed the limits of this paper. At the same time, it is well known that the interaction of electrons with I-phonons is negligibly low in wide quantum wells, so that the theory developed here has an independent value for such nanosystems.

2.3. Hamiltonian of the electron-phonon system and Green's function of an electron in 3BRTS

The Hamiltonian

$$\hat{H} = \hat{H}_e + \hat{H}_L + \hat{H}_{e-L} \tag{22}$$

obtained for the electron-phonon system in the 3BRTS allows the Fourier transform of the electron Green's function to be calculated analytically for an arbitrary temperature of the system following the procedure of the Feynman–Pines diagram technique [16, 25], provided that the average occupation numbers of electron states are small ($n_\mathbf{k} \ll 1$), and those

1194

of phonon states are determined by the Bose–Einstein distribution

$$\nu_{j\ell} = \left(e^{\frac{\Omega_{j\ell}}{k_B T}} - 1 \right)^{-1}. \tag{23}$$

In this case, the Fourier transform of the electron Green's function is determined by the Dyson equation [16, 24]

$$G_n(\mathbf{k}, E) = \{E - E_{n\mathbf{k}} - M_n(\mathbf{k}, E)\}^{-1}, \tag{24}$$

in which, while considering the mass operator $M_n(\mathbf{k}, E)$, it is enough to confine the diagram series to the one-phonon approximation,

$$M_n(\mathbf{k}, E) = \sum_{j=1}^{5} \sum_{n'=1}^{N} \sum_{\ell, \lambda, \mathbf{q}} f_{nn'}^{j\lambda *}(\ell) f_{n'n}^{j\lambda}(\ell) \times$$

$$\times d_j^2 S^{-1} \left\{ \frac{1 + \nu_{j\ell}}{E - E_{n'}(\mathbf{k} + \mathbf{q}) - \Omega_{j\ell} + i\eta} + \right.$$

$$\left. + \frac{\nu_{j\ell}}{E - E_{n'}(\mathbf{k} + \mathbf{q}) + \Omega_{j\ell} + i\eta} \right\}. \tag{25}$$

Here, N is the number of energy bands (levels) in the potential wells of the nanosystem. The substitution of the summation over the two-dimensional quasi-momentum $\mathbf{q}$ by the integrals ($\sum_{\mathbf{q}} \Rightarrow (2\pi)^{-2} S \times \iint d^2 \mathbf{q}$) in the polar coordinate system allows one to exactly (analytically) calculate the mass operator (25) at $\mathbf{k} = 0$, which corresponds to a typical experimental situation, where electrons move normally to the heterosystem surface. As a result, for the quantity $M_n(\mathbf{k} = 0, E)$, we obtain

$$M_n(\mathbf{k}, E) = -\sum_{j=1}^{5} \sum_{n'=1}^{N} \sum_{\lambda, \ell} \left(\frac{2\hbar^2}{m_n^* d_j^2} \right)^{-1} d_j^2 S^{-1} \times$$

$$\times f_{nn'}^{j\lambda *}(\ell) f_{n'n}^{j\lambda}(\ell) \int_0^\infty \frac{dx}{\pi^2 \lambda^2 + \left(\frac{\hbar^2}{2m_n^* d_j^2} \right)^{-1} x} \times$$

$$\times \left\{ \frac{1 + \nu_{j\ell}}{x + E_{n'} + \Omega_{j\ell} - E + i\eta} + \right.$$

$$\left. + \frac{\nu_{j\ell}}{x + E_{n'} - \Omega_{j\ell} - E + i\eta} \right\}, \quad (\eta \to +0). \tag{26}$$

Taking the weakness of the electron-phonon coupling into account, putting $E = E_n$ in the mass operator, and extracting the real,

$$\Delta_n = \Delta_{nn} + \sum_{n' \neq n} \Delta_{nn'} =$$

$$= \text{Re} M_{nn}(E_n) + \sum_{n' \neq n} \text{Re} M_{nn'}(E_n), \tag{27}$$

and imaginary,

$$\Gamma_n = \Gamma_{nn} + \sum_{n' \neq n} \Gamma_{nn'} =$$

$$= 2\text{Im} M_{nn}(E_n) + 2 \sum_{n' \neq n} \text{Im} M_{nn'}(E_n), \tag{28}$$

parts, which describe the total shift Δ_n and the damping Γ_n, respectively, for the n-th band, as well as their partial intraband (Δ_{nn} and Γ_{nn}) and interband ($\Delta_{nn' \neq n}$ and $\Gamma_{nn' \neq n}$) components, after the exact analytical integration, we obtain

$$\Delta_n = \Delta_n^+ + \Delta_n^- =$$

$$= (\Delta_{nn}^+ + \sum_{n' \neq n} \Delta_{nn'}^+) + (\Delta_{nn}^- + \sum_{n' \neq n} \Delta_{nn'}^-), \tag{29}$$

$$\Gamma_n = \Gamma_n^+ + \Gamma_n^- =$$

$$= (\Gamma_{nn}^+ + \sum_{n' \neq n} \Gamma_{nn'}^+) + (\Gamma_{nn}^- + \sum_{n' \neq n} \Gamma_{nn'}^-), \tag{30}$$

where

$$\Delta_n^\pm = -\sum_{n'=1}^{N} \sum_{j, \lambda, \ell} \left(\frac{2\pi \hbar^2}{m_n^* d_j^2} \right)^{-1} f_{nn'}^{j\lambda *}(\ell) f_{n'n}^{j\lambda}(\ell) \times$$

$$\times \ln \left[\frac{(\pi \lambda \hbar)^2}{2m_n^* d_j^2 |E_{n'} - E_n \pm \Omega_{j\ell}|} \right] \left\{ \begin{matrix} 1 + \nu_{j\ell} \\ \nu_{j\ell} \end{matrix} \right\} \times$$

$$\times \left\{ \frac{\Theta(E_{n'} - E_n \pm \Omega_{j\ell})}{(\pi \lambda)^2 - |E_{n'} - E_n \pm \Omega_{j\ell}| \left(\frac{\hbar^2}{2m_n^* d_j^2} \right)^{-1}} + \right.$$

$$\left. + \frac{\Theta(E_n - E_{n'} \pm \Omega_{j\ell})}{(\pi \lambda)^2 + |E_{n'} - E_n \pm \Omega_{j\ell}| \left(\frac{\hbar^2}{2m_n^* d_j^2} \right)^{-1}} \right\}, \tag{31}$$

Physical parameters of nanosystem components

	ε_∞	$\hbar\omega_{L1}$, meV	$\hbar\omega_{T1}$, meV	$\hbar\omega_{L2}$, meV	$\hbar\omega_{T2}$, meV	m, m_e	U, meV
GaAs	10.89	36.25	33.29			0.067	$0.6\,(1266x + 260x^2)$
$Al_xGa_{1-x}As$	$10.89 - 2.73x$	$36.25 - 6.553x +$ $+ 1.793x^2$	$33.29 - 0.643x -$ $- 1.163x^2$	$44.63 + 8.783x -$ $- 3.323x^2$	$44.63 + 0.553x -$ $- 0.303x^2$	$0.067 +$ $+ 0.083x$	

$$\Gamma_n^\pm = \sum_{n'=1}^N \sum_{j,\lambda,\ell} \left(\frac{4\hbar^2}{m_n^* d_j^2}\right)^{-1} f_{nn'}^{j\lambda*}(\ell) f_{n'n}^{j\lambda}(\ell) \times$$

$$\times \frac{\Theta(E_n - E_{n'} \pm \Omega_{j\ell}) \begin{Bmatrix} 1 + \nu_{j\ell} \\ \nu_{j\ell} \end{Bmatrix}}{(\pi\lambda)^2 + |E_{n'} - E_n \pm \Omega_{j\ell}| \left(\frac{\hbar^2}{2m_n^* d_j^2}\right)^{-1}}. \tag{32}$$

The theory developed here allows one to calculate and analyze the parameters of electron spectrum in the 3BRTS renormalized by the electron interaction with confined L-phonons at given physical and geometrical parameters of the system.

3. Analysis of the Temperature and Content Dependences of the Electron Spectrum Parameters Using 3BRTSs with GaAs Wells and $Al_xGa_{1-x}As$ Barriers as an Example

The shifts and the damping of the electron spectrum in the 3BRTS were calculated taking a 3BRTS $GaAs/Al_xGa_{1-x}As$ as an example. This structure is an active zone in experimentally studied QCDs [21,22]. The physical parameters of the elements composing the system are quoted in Table.

In Fig. 2, the dependences of the electron spectral parameters on the internal barrier position a_1 between the external ones are depicted for two 3BRTSs with the identical total widths of both wells ($a = a_1 + a_2 = 13.9$ nm), provided that the width of the internal barrier is fixed ($b = 1.13$ nm), but the Al contents in all barriers are different: (A) $x = 0.15$, and the potential barrier is low, $U = 120$ meV (panels a to c); and (B) $x = 0.45$, and the potential barrier is high, $U = 320$ meV (panels d to f). The temperature $T = 0$ K. One can see that, irrespective of the Al content x in the RTS layer-barriers, the dependences of all electron spectral parameters on the width a_1 of the first layer-well are qualitatively similar and symmetric with respect to the 3BRTS

middlepoint $a_1 = a/2$. In the 3BRTS A with shallow wells ($x = 0.15$), there are three quasi-stationary states. The energies of two working states (E_1 and E_2) are located below the corresponding energies in the 3BRTS B with deep wells ($x = 0.45$), which is characterized by four quasi-stationary states (Fig. 2, panels a and d).

The energy of the quantum transition between two lowest levels ($E_{21} = E_2 - E_1$), which is accompanied by the absorption of the electromagnetic field, depends nonlinearly on the size a_1 of the first well. As a_1 increases from zero to about $a_1/4$, the magnitude of E_{21} increases and reaches the maximum value max $E_{21} = 48$ (A) or 76 meV (B). As a_1 increases further, E_{21} decreases and reaches the minimum value: min $E_{21} = 29$ (A) or 20 meV (B) at $a_1 = a/2$.

Owing to the interaction of electrons with virtual phonons, the total negative shift Δ_1 of the first working level decreases as a_1 grows within the interval $0 \leq a_1 \leq a/2$. Almost at all a_1-values, its magnitude is mainly formed by the intraband interaction (Δ_{11}), because the partial contributions of the electron interaction with phonons through other bands are rather small; only in a vicinity of $a_1 \approx a/2$, their total contribution to the shift, $\Delta_{1\Sigma} = \sum_{n' \neq n} \Delta_{1n'}$, is comparable with the magnitude of Δ_{11}.

The total negative shift Δ_2 of the second working level (Figs. 2, c and f) decreases, as a_1 increases within the interval $0 \leq a_1 \leq a/4$, increases in the interval $a/4 \leq a_1 \leq a/3$, and becomes weakly nonlinear in the interval $a/3 \leq a_1 \leq a/2$. For system A with a_1 within the interval $0 \leq a_1 \leq a/3$ (Fig. 2, c), the total contribution $\Delta_{2\Sigma}$ of the interband interaction to the shift Δ_2 is comparable with the contribution Δ_{22} of the intraband interaction, but is almost twice as large as Δ_{22} within the interval $a/3 \leq a_1 \leq a/2$. For system B (Fig. 2,f), the contributions Δ_{22} and $\Delta_{2\Sigma}$ to the magnitude of Δ_2 are comparable at all a_1-values.
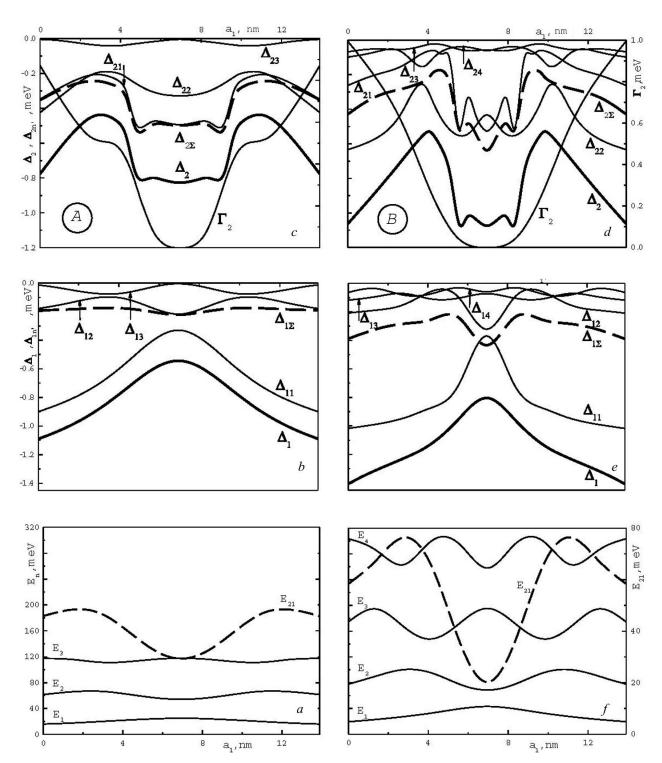
1196

Fig. 2. Dependences of electron spectral parameters on the position a_1 of the internal barrier between external 3BRTS barriers at $T = 0$ K
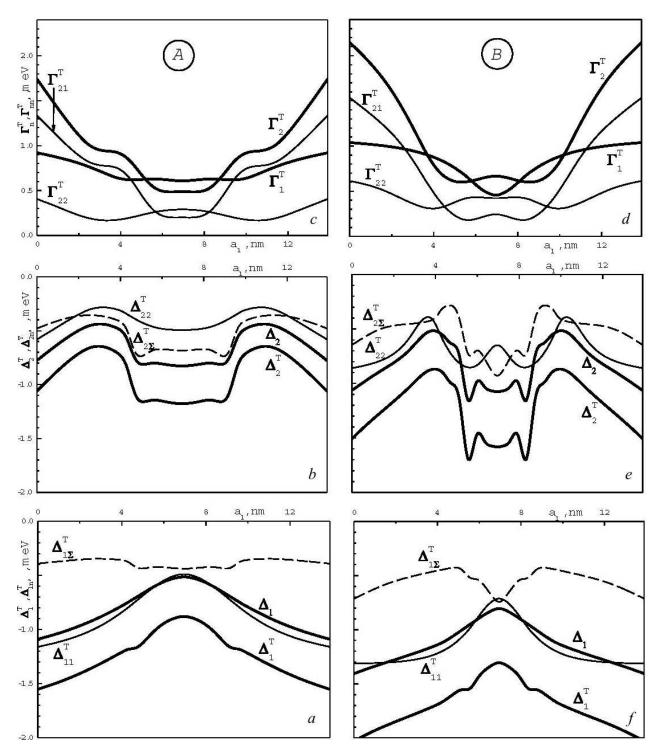
Fig. 3. Dependences of electron spectral parameters on the position a_1 of the internal barrier between external 3BRTS barriers at $T = 300$ K

Concerning the damping Γ_2 (Figs. 2, *c* and *f*), if $T = 0$ K, it arises only in the second working state ($\Gamma_2 = \Gamma_{21}$) because of the interband interaction of electrons in this state with the electrons in the first (ground) state by means of virtual phonons, provided that $E_2 > E_1 + \Omega_{j\ell}$. Certainly, the intra- and interband interactions of electrons in the lower (in particular, the ground) states with the electrons in the higher excited states by means of phonons do not result in the damping in accordance with the physical reasoning.

The temperature dependences of spectral parameters, as is seen from the mass operator (26), is governed by the average values of occupation numbers, ν, of phonon states in the processes of electron-phonon interaction with the phonon emission (the first term in the mass operator) and absorption (the second term in the mass operator). In Fig. 3, the evolution of the total, $\Delta_n^T = \Delta_n + \Delta_n(T)$, and partial, $\Delta_{nn}^T = \Delta_{nn} + \Delta_{nn}(T)$ and $\Delta_{n\Sigma}^T = \Delta_{n\Sigma} + \Delta_{n\Sigma}(T)$, shifts, and the total, $\Gamma_n^T = \Gamma_n + \Gamma_n(T)$, and partial, $\Gamma_{nn}^T = \Gamma_{nn} + \Gamma_{nn}(T)$ and $\Gamma_{n\Sigma}^T = \Gamma_{n\Sigma} + \Gamma_{n\Sigma}(T)$, widths with the variation of the internal barrier position a_1 with respect to the external barriers in the 3BRTS at the temperature $T = 300$ K is shown. The figure demonstrates that the contributions made by real phonons to the magnitudes of total, Δ_n^T, and partial shifts and total, Γ_n^T, and partial widths at $T = 300$ K are comparable with the contribution Δ_n made by virtual phonons at $T = 0$ K. The qualitative dependences of those quantities on the internal barrier position a_1 also remains similar to that obtained at $T = 0$ K. In addition, irrespective of the Al content x and the value of a_1, when the temperature increases to 300 K, the absolute values of all renormalizing spectral parameters in system A grow a bit less than in system B. It is also worth noting that, at nonzero temperatures, owing to the processes of real photon absorption (since $\nu \neq 0$), the damping arose not only in the excited but also in the ground electron state (Figs. 3, *c* and *f*).

4. Conclusions

The Hamiltonian of a system of electrons that interact with confined polarization phonons in a nano-3BRTS with three-component barriers was obtained for the first time in the second-quantization representation for all variables.

The temperature Green's function technique is used to calculate and analyze the phonon-renormalized shifts and the damping of two lowest (working) electron states in the 3BRTS GaAs/Al$_x$Ga$_{1-x}$As at $T = 0$ and 300 K.

It is shown that, independently of the temperature and the Al content in barriers, the variation of the internal barrier position brings about a nonlinear evolution of the damping and negative shifts of electron states.

The developed approach makes it possible to consider other mechanisms of electron interaction (electron-to-electron, with the interface polarization and acoustic phonons, with dc electric and high-frequency electromagnetic fields). The elaborated theory, involving the main mechanisms of interaction between electrons at their tunneling through open multilayered RTSs, will allow not only the physical phenomena in nanoheterosystems to be studied in detail, but also the operational characteristics of QCDs, QCLs, and others nanodevices to be optimized.

1. J. Faist, F. Capasso, D.L. Sivco, C. Sirtori, A.L. Hutchinson, and A.Y. Cho, Science **264**, 533 (1994).
2. J. Faist, F. Capasso, C. Sirtori, D.L. Sivco, A.L. Hutchinson, and A.Y. Cho, Appl. Phys. Lett. **66**, 538 (1995).
3. C. Gmachl, F. Capasso, D.L. Sivco, and A.Y. Cho, Rep. Prog. Phys. **64**, 1533 (2001).
4. D. Hofstetter, M. Beck, and J. Faist, Appl. Phys. Lett. **81**, 2683 (2002).
5. L. Gendron, M. Carras, A. Huynh, V. Ortiz, C. Koeniguer, and V. Berger, Appl. Phys. Lett. **85**, 2824 (2004).
6. F.R. Giorgetta, E. Baumann, D. Hofstetter, C. Manz, Q. Yang, K. Köhler, and M. Graf, Appl. Phys. Lett. **91**, 111115 (2007).
7. K. Ning, Q-U. Liu, L. Lu *et al.*, Chin. Phys. Lett. **27**, 12850 (2010).
8. V.F. Elesin and Yu.V. Kopaev, Zh. Eksp. Teor. Fiz. **123**, 1308 (2003).
9. A.B. Pashkovskii, Pis'ma Zh. Eksp. Teor. Fiz. **89**, 32 (2009).
10. M.V. Tkach and Yu.O. Seti, Ukr. Fiz. Zh. **58**, 182 (2013).
11. G.G. Zegrya, M.V. Tkach, and Yu.O. Seti, Fiz. Tverd. Tela **55**, 2067 (2013).
12. M.V. Tkach, Ju.O. Seti, I.V. Boyko, and O.M. Voitsekhivska, Rom. Rep. Phys. **65**, 1443 (2013).
13. F.R. Giorgetta *et al.*, IEEE J. Quant. Electr. **45**, 1039 (2009).
14. S. Yarlagadda, Int. J. Mod. Phys. B **15**, 3529 (2001).

15. M. Tkach, V. Holovatsky, O. Voitsekhivska, M. Mykhalyo-va, and R. Fartushynsky, Phys. Status Solidi B **225**, 331 (2001).

16. M.V. Tkach, *Quasiparticles in Nanoheterosystems* (Ruta, Chernivtsi, 2003) (in Ukrainian).

17. X. Gao, D. Botez, and I. Knezevic, J. Appl. Phys. **103**, 073101 (2008).

18. J.G. Zhu and S.L. Ban, Eur. Phys. J. B **85**, 140 (2012).

19. N. Mori and T. Ando, Phys.Rev. B **40**, 6175 (1989).

20. K.W. Kim and M.A. Stroscio, Appl. Phys. J. **68**, 6289 (1990).

21. B.H. Wu, J.C. Cao, G.Q. Xia, and H.C. Liu, Eur. Phys. J. B **33**, 9 (2003).

22. H. Luo, H.C. Liu, C.Y. Song, and Z.R. Wasilewski, Appl. Phys. Lett. **86**, 231103 (2005).

23. C.H. Yu *et al.*, Appl. Phys. Lett. **97**, 022102 (2010).

24. A.S. Davydov, *Quantum Mechanics* (Pergamon Press, New York, 1976).

25. A.A. Abrikosov, L.P. Gor'kov, and I.E. Dzyaloshinskii, *Methods of Quantum Field Theory in Statistical Physics* (Prentice Hall, Englewood Cliffs, N.J., 1963).

М.В. Ткач, Ю.О. Сеті, Ю.Б. Гринишин

ВПЛИВ ОБМЕЖЕНИХ
ПОЛЯРИЗАЦІЙНИХ ФОНОНІВ НА ЕЛЕКТРОННИЙ
СПЕКТР ТРИБАР'ЄРНОЇ АКТИВНОЇ ЗОНИ
КВАНТОВОГО КАСКАДНОГО ДЕТЕКТОРА

Р е з ю м е

У моделі ефективних мас і прямокутних потенціалів для електронів та в моделі поляризаційного континууму для обмежених фононів у трибар'єрній резонансно-тунельній наноструктурі отримано гамільтоніан електрон-фононної системи у зображенні чисел заповнення за всіма змінними. Методом функцій Гріна розраховано перенормований спектр електронів у трибар'єрній резонансно-тунельній наноструктурі на основі GaAs-ям і $Al_xGa_{1-x}As$-бар'єрів при різних значеннях концентрації (x) Al. Встановлено, що при зміні температури від 0 до 300 K, незалежно від концентрації Al, зі зміною геометричної конфігурації трибар'єрної резонансно-тунельної наноструктури ширини обох нижніх (робочих) квазістаціонарних станів збільшуються, а енергії зміщуються у низькоенергетичну область. Ширини і зміщення виявилися сильно нелінійними функціями у залежності від положення внутрішнього бар'єра в трибар'єрній резонансно-тунельній наноструктурі.